

## **Characterizing Piezoresistive Smart Cement Modified with Silicon Dioxide Nanoparticles Using Vipulanandan Models for Multiple Applications**

**Professor C. Vipulanandan Ph.D., P.E.**

“Smart Cement” Inventor and Text Book

“Vipulanandan Rheological Model”

“Vipulanandan Failure Model”

Chief Editor – Advances in Civil Engineering

Director, Center for Innovative Grouting Material and Technology (CIGMAT)

Director, Texas Hurricane Center for Innovative Technology (THC-IT)

Professor of Civil and Environmental Engineering

University of Houston, Houston, Texas 77204-4003

### **Abstract**

In this study, highly sensing chemo-thermo- piezoresistive smart cement was modified with up to 1% silicon dioxide nanoparticles (Nano Silica - $\text{NanoSiO}_2$ ) to evaluate the effects not only on the sensing properties but also the compressive stress-strain relationship, strength and modulus. The oil well cement (class H) and cement modified with  $\text{NanoSiO}_2$  were characterized using the X-ray diffraction analysis (XRD) and thermal gravimetric analysis (TGA). Smart cement was prepared by adding 0.1% carbon fibers (CF) based on the cement weight and new Vipulanandan piezoresistive theory to make the cement a piezoresistive but still a nonconductive material. Testing evaluated the smart cement behavior with and without  $\text{NanoSiO}_2$  in order to verify the sensitivity of electrical resistivity changes with curing time and compressive loading. The addition of 0.5% and 1%  $\text{NanoSiO}_2$  increased the initial electrical resistivity of the smart cement by 17% and 35% respectively, hence electrical resistivity a material property that can be used as a quality control parameter for mixing in the field. In a one day, the maximum change in the electrical resistivity (index  $\text{RI}_{24\text{hr}}$ ) for the smart cement without  $\text{NanoSiO}_2$  was 364%. The  $\text{RI}_{24\text{hr}}$  for the smart cement with  $\text{NanoSiO}_2$  addition decreased and the change was depended on the amount of  $\text{NanoSiO}_2$ . The addition of 1%  $\text{NanoSiO}_2$  increased the compressive strength of the smart cement by 14% and 42% after 1 day and 28 days of curing respectively. With 1%  $\text{NanoSiO}_2$  addition the compressive modulus of the smart cement increased by 100%. This is another clear indication of chemical reaction between the  $\text{NanoSiO}_2$  and hydrating cement products. The Vipulanandan p-q curing model predicted the changes in electrical resistivity with curing time very well. The smart cement piezoresistive axial strain at failure with  $\text{NanoSiO}_2$  was over 500 times higher than the regular cement depending on the curing time and  $\text{NanoSiO}_2$  content. But the piezoresistive axial strain at failure for the smart cement reduced with the addition of  $\text{NanoSiO}_2$ . The Vipulanandan p-q stress-strain model and stress- piezoresistive strain model also predicted the experimental results very well. For the smart cement modified with  $\text{NanoSiO}_2$ , the resistivity change at peak stress was over 1250 times (125,000%) higher than the change in the compressive strain. Also a linear correlation was obtained between the  $\text{RI}_{24\text{hr}}$  and the compressive strength of the  $\text{NanoSiO}_2$  modified smart cement based on the curing time.

## Introduction

In the construction industry and petroleum industry, cement has been used for multiple applications and there is need for further enhancement of the sensing properties and mechanical properties of the cement. In the construction industry it is used a binder in various types of grouts and concrete to construct deep foundations, pipes, bridges, highways, storage facilities and buildings. In the oil industry cement is typically utilized to fill the annular space between the casing and rock formation by displacing the drilling fluid. Also cement will support the casing and protect it against corrosion and impact loading, restrict the movement of fluids between formations, and isolate productive and nonproductive zones. Oil well cement is used under different conditions of exposures compared to the cement used in the conventional construction industry. The strength of oil well cement usually depends on factors such as time and conditions of curing, environmental conditions, slurry design and use of additives and any additional treatments to the cement. One of the important additive that has been used in cement is silica, which has been used in a certain amount to mitigate the strength degradation (Choolaei et al. 2012; Quercia et al. 2016). As deep-water exploration and production of oil and gas expand around the world, there are unique challenges in good construction beginning at the seafloor. Also, preventing the loss of fluids to the formations and proper well cementing have become critical issues in good construction to ensure wellbore integrity because of varying downhole conditions (Labibzadeh et al. 2010, Vipulanandan 2021). Moreover, the real-time monitoring of the changes in the cement in-situ is critical to evaluate the performance of the cemented wells (Vipulanandan et al. 2015a). Foremost important among these is to form a sealing layer between the well casing and the geological formation, referred to as the zonal isolation. With some of the reported failures and growing interest in addressing environmental and economic concerns in the oil and gas industry, the integrity of the cement sheath is of major importance. Recent case studies on cementing failures have clearly identified several issues that resulted in various types of delays in the cementing operations. Also preventing the loss of fluids to the formations and proper well cementing have become critical issues in well construction to ensure wellbore integrity because of varying downhole conditions (Vipulanandan et al. 2015a, 2016, 2021). The catastrophic accident in the Gulf of Mexico in April 2010 was one of the world's worst oil spills (Izon et al. 2007, Vipulanandan 2021). Two studies performed during the period of 1971 to 1991 and 1992 to 2006 clearly identified cement failures as the major cause for blowouts. Cementing failures increased significantly during the second period of study when 18 of the 39 blowouts were due to the cementing problem and over 50% of the blowouts controlled by pumping mud or cement or by actuating mechanical well control equipment (Izon et al. 2007). Therefore, proper monitoring and tracking the entire process of well cement become important to ensure cement integrity during the service life of the well (Vipulanandan et al. 2017).

Electrical resistivity measurement has been applied by many researchers related to concrete and cement applications (McCarter et al. 2000 and 2003). Electrical response characteristics measurement has appropriate sensitivity in monitoring the characteristics of cementitious materials (Han et al. 2007 and 2016). The advantages of using this technique include its accuracy, easy test procedure, and nondestructive characteristics (Mohammed 2016). Additionally, this method can be used for monitoring the long-term behavior of cement in practice. The electrical resistivity of cement is affected by a number of factors such as pore structure (continuity and tortuosity), pore solution composition, cementitious content, water-to-cement ratio, moisture content, and

temperature (Mangadlao et al. 2015; Vipulanandan et al. 2018a). Moreover, the electrical resistivity of cement is dramatically affected by contaminations, due to the resistivity contrast between cement and the contaminating substance. Study by Han et al. (2007, 2016) investigated the piezoresistivity of cement-based material with carbon fiber and carbon black under monotonic and repeated compressive loadings, and was found that the piezoresistivity of the modified cement was reversible and stable within the elastic regime. In this study up to 3% (by volume) of carbon fiber was used and it reduced the electrical resistivity of the cement and hence making it more conductive and vulnerable to corrosion. Also applying the compressive stress further reduced the electrical resistivity by about 30% at peak stress and making the material more conductive. Vipulanandan et al. (2015 (a) and (b); 2016; 2017; 2018 (a) and (b), 2021), developed piezoresistive materials using the percolation theory and have shown that the changes in electrical resistivity increased with the applied compressive or tensile stress in both cementitious and polymeric composites because the changes in resistivity was influenced by the deviatoric stress. These studies have also shown that the changes in resistivity in the materials at the peak stresses were 30 to 2800 times higher than the strain in the materials. Hence, instead strain, the change in resistivity has the potential to be used to determine the integrity of the materials. A new method has been developed to measure the electrical resistivity of the materials using the two probe method with alternative current. LCR meters (measures the inductance (L), capacitance (C) and resistance (R)) were used at 300 kHz frequency to measure the changes in the bulk resistance (Vipulanandan et al. 2021). A field well was installed and cemented using the smart cement mixture with enhanced piezoresistive properties (Vipulanandan et al. 2021). The field well was designed, built, and used to demonstrate the concept of real time monitoring of the flow of drilling mud and smart cement and hardening of the cement in place. Change in the resistance of hardening cement was continuously monitored since the installation of the field well for over 7 years (Vipulanandan et al. 2021). The pressure testing showed the piezoresistive response of the hardened smart cement and a piezoresistive model has been developed to predict the pressure in the casing from the change in resistivity in the smart cement (Vipulanandan et al. 2021).

Use of nanoparticles in the areas of medicine, science and engineering are rapidly increasing because of multiple benefits based on the size, shape and chemical compositions of the nanoparticles. With the advancement of nanotechnology, several of these materials can be used to solve some of the problems encountered in cementing (Vipulanandan et al. 2021).

### **NanoSiO<sub>2</sub>**

Nanosilica is a versatile nanomaterial suitable as drug carriers in medicine, fillers in polymers and fertilizer/pesticide carriers and potentially bioavailable source of silicon in agriculture. Based on the improved compressive strength, it is clear that NanoSiO<sub>2</sub> behaves not only as a filler to improve the cement microstructure, but also to promote the pozzolanic reactions (Choolaei et al. 2012; Singh et al. 2013). Therefore, it is of interest to add NanoSiO<sub>2</sub> particles to the cement mixtures to enhance the performance of cement and concrete. Also the effects of NanoSiO<sub>2</sub> on the performance of cement under various types of applications have been documented in the literature by several researchers in the past decade (Singh et al. 2013).

Nano-scaled silica particles have a filler effect by filling up the voids between the cement grains. With the right composition, the higher packing density results in a lower water demand of the mixture and it also contributes to strength enhancement due to the reduced capillary porosity.

## Objective

The overall objective of this study was to investigate the effect of up to 1% of NanoSiO<sub>2</sub> on the modified smart cement (Class H) behavior. The specific objectives were as follows:

- i. Evaluation the effect of NanoSiO<sub>2</sub> on the oil well cement using X-Ray diffraction and thermogravimetric analysis (TGA).
- ii. Investigate and quantify the changes in the electrical resistivity during the curing time and compressive behavior of the NanoSiO<sub>2</sub> modified smart cement.
- iii. Model the curing, compressive stress-strain, and compressive piezoresistive behavior of the NanoSiO<sub>2</sub> modified smart cement.

## Materials and Methods

### Silicon dioxide nanoparticle (NanoSiO<sub>2</sub>)

Silicon dioxide nano powder (NanoSiO<sub>2</sub>) with the grain size of 12 nm, specific surface area of 175 to 225 m<sup>2</sup>/g (from supplier datasheet) was selected for this study.

### Smart Cement Sample

In this study, smart well cement (Class H) with water-to-cement (w/c) ratio of 0.38 was used. The samples were prepared according to the API standards. To improve the sensing properties and piezoresistive behavior of the smart cement, it was modified with 0.1% of conductive fillers (CF) by weight of cement and mixed in all of the samples. Three series of smart cement slurries were prepared with NanoSiO<sub>2</sub> up to 1 % (by the weight of the cement) and tested up to 28 days of curing.

Total of 0.1 % of carbon fibers (CF) was added with the cement mix as the base modification. The CF used in this study was about 10 μm in diameter. NanoSiO<sub>2</sub> was added to the smart cement in the mixer with the mixing intervals of 20 sec at 4000 rpm. Cement, water, and additives (0.1% CF and NanoSiO<sub>2</sub>) were mixed at the speed of 4000 rpm for 3 minutes and 35 seconds at the speed of 1200 rpm. The two wires were placed in the mold and the vertical distance between the two wires were 50 mm. The embedment depth of the wire in the specimen was about 25 mm. For setting time monitoring and compressive stress tests, cylinders with the diameter of 50 mm (2 inches) and a height of 100 mm (4 inches) were prepared. For quick property changes monitoring, a two-probe method was selected. During the initial stages of setting, conductivity and API resistivity meters were used to determine the curing cement resistivity and using Eqn. (1) the calibration parameter K was obtained with time (Vipulanandan and Mohammed 2015(b)). The average value of parameter K was 56.5 m<sup>-1</sup>. In order to have consistent result, at least three specimens were prepared for each type of mix.

### XRD analysis

An X-ray diffraction (XRD) analyses was performed in order to determine the chemical composition of the cement at 25°C. The powder (≈2 g) was placed in an acrylic sample holder (3

mm) depth. The samples were analyzed by using parallel beam optics with  $\text{CuK}\alpha$  radiation at 40 kV and 30 mA. The samples were scanned for reflections ( $2\theta$ ) from  $0^\circ$  to  $90^\circ$  in steps of  $0.02^\circ$  and a 2 sec count time per step.

### **Thermogravimetric analysis (TGA)**

Thermogravimetric analysis curves, mass loss (TGA) and its derivative (DTG) were quantified using a Setaram TGA 500 apparatus at a heating rate of  $10^\circ\text{C}/\text{min}$  for a mass sample of about 20 mg. The sample was loaded in a platinum pan ( $\frac{3}{4}$  full). This was followed by the introduction of  $\text{N}_2$  gas into the TGA compartment for 5 minutes to purge the likely oxygen in the environment of the system. After the purging, the sample was heated in the  $\text{N}_2$  atmosphere from room temperature to the maximum of  $800^\circ\text{C}$ . The weight loss percentage and temperature relationships were obtained for the samples. In this study, the (TGA) and (DTG) curves were obtained for cement,  $\text{NanoSiO}_2$  and cement modified with 1% of  $\text{NanoSiO}_2$  after 7 days of curing.

### **Density**

Density of smart cement with and without  $\text{NanoSiO}_2$  was measured immediately after mixing using the standard mud balance cup.

### **Electrical resistivity**

Two different instruments were used to measure the electrical resistivity of the smart cement:

#### **(i). Conductivity probe**

A commercially available conductivity probe was used to measure the conductivity (inverse of electrical resistivity) of the cement slurry. The conductivity measuring range was  $10,000\ \Omega\text{-m}$  to  $0.1\ \Omega\text{-m}$ .

#### **(ii) Digital resistivity meter**

An API resistivity meter measured the resistivity of fluids, slurries, and semi-solids with resistivities in the range of  $0.01\ \Omega\text{-m}$  to  $400\ \Omega\text{-m}$ . Both of the electrical resistivity devices were calibrated using standard solutions of sodium chloride ( $\text{NaCl}$ ).

Based on past studies, electrical resistivity was selected as a monitoring parameter to quantify the performance of modified cement during curing and hardening process. The electrical resistivity of the slurries was measured using an API standard resistivity meter. Further, electrical resistance was measured using an inductance, capacitance, and resistance (LCR) meter during the curing time. To minimize the contact resistances, the resistance was measured at 300 kHz using the two-wire method. Each specimen was calibrated to obtain the electrical resistivity ( $\rho$ ) from the measured electrical resistance ( $R$ ) based on the Eqn.1 (Vipulanandan et al. 2021).

$$R = \rho * \left(\frac{L}{A}\right) = \rho K \quad (1)$$

where  $L$  is the distance between the wires,  $A$  is the cross-sectional area through which the current is flowing, and  $L/A$  is called the nominal geometry factor. In insulator material, such as cement,

the actual pathway of the current is not well defined as compared to the conductive material such as metals. Hence,  $L/A$  in Eqn. (1) was replaced by an experimentally determined calibration factor ( $K$ ), by measuring the bulk resistance ( $R$ ) and the resistivity ( $\rho$ ) of the material at the same time (Vipulanandan 2021). Also normalized change in resistivity with the changing conditions (curing, stress) can be represented as follows:

$$\frac{\Delta\rho}{\rho} = \frac{\Delta R}{R} \quad (2)$$

In this study modified cement materials are represented in terms of resistivity ( $\rho$ ) to the changes (composition, curing and stress) since it has been shown to be a sensitive parameter (Vipulanandan 2021).

### **Compressive strength test (ASTM C 39)**

The cylindrical specimen with the diameter of 2 inches and a height of 4 inches (50mm Dia.\*100 mm height) was capped (sulfur capping) and tested at a predetermined controlled displacement rate. Compression tests were performed on cement samples after 1 day, 7 days and 28 days of curing using a hydraulic compression testing machine. Also 10 mm in length strain gages with initial resistance of 120  $\Omega$  were used to measure the axial strain.

### **Piezoresistivity test**

Piezoresistivity describes the change in the electrical resistivity of a material under pressure. Since oil well cement serves as the pressure-bearing part of wells in real applications, the piezoresistivity of modified and unmodified cement was investigated under compressive loading. During compression testing, electrical resistance was measured in the stress axis. To eliminate the polarization effect, alternating current resistance measurements were made using a LCR meter at a frequency of 300 kHz.

### **Nonlinear model parameters (NLM)**

The electrical resistivity ( $\rho$ ) of the smart cement slurry modified with silica nanoparticle ( $\text{NanoSiO}_2$ ) was influenced by the composition of the cement and curing time ( $t$  (day)). It is being proposed to relate the model parameters to the independent variables (curing time and  $\text{NanoSiO}_2$  content) using a nonlinear power relationship (Vipulanandan and Mohammed 2015 a). Hence the effects of curing time ( $t$ ) and  $\text{NanoSiO}_2$  content on the model parameters were determined using the non-linear model (NLM) (Vipulanandan et al. 2015a) as follows:

$$\text{Model parameters} = a * (t)^b + c * (t)^d * (\text{NanoSiO}_2(\%))^e \quad (3)$$

The NLM parameters ( $a$ ,  $b$ ,  $c$ ,  $d$ ,  $e$ ) will be obtained from multiple regression analyses using the least square method.

## **Results and Discussion**

### **X-ray Analyses**

#### **(a). Cement**

The XRD pattern of Class H cement is shown in Figure 1 (a). The major constituents in the cement included tricalcium silicate ( $\text{Ca}_3\text{SiO}_5$ ), dicalcium silicate ( $\text{Ca}_2\text{SiO}_4$ ), calcium aluminoferrite ( $\text{Ca}_2\text{FeAlO}_5$ ), calcium sulfate ( $\text{CaSO}_4$ ), quartz ( $\text{SiO}_2$ ) and magnesium sulfate ( $\text{MgSO}_4$ ).

### **(b). Cement with 1% NanoSiO<sub>2</sub>**

Addition of 1% NanoSiO<sub>2</sub> modified the cement composition after 7 days of curing with the formation of magnesium silicate sulfate ( $\text{Mg}_5(\text{SiO}_4)_2\text{SO}_4$ : Ma) ( $2\theta$  peaks at  $51.58^\circ$  and  $56.50^\circ$ ) and also adding more quartz ( $\text{SiO}_2$ ) ( $2\theta$  peaks at  $23.55^\circ$ ,  $36.90^\circ$  and  $62.50^\circ$ : Q) based on XRD intensity as shown in Figure 1 (b). Adding NanoSiO<sub>2</sub> to the cement resulted in mineralogy changes and it is important to investigate these changes on the smart cement behavior.

### **TGA analyses**

The thermogravimetric analyses (TGA) and differential thermogravimetric (DTG) results were obtained for the oil well cement, silica nanoparticle (NanoSiO<sub>2</sub>) and cement modified with 1% NanoSiO<sub>2</sub> after 7 days of curing as summarized in Table 1 and also shown in Figure 2. The heating rate used in these tests was  $10^\circ\text{C}/\text{min}$  which also shows weight loss at  $110^\circ\text{C}$  (standard temperature for determining free water), as shown in Figure 2. Four characteristic endothermic effects were observed as summarized in Table 1. The initial effect, in the temperature range from  $25^\circ\text{C}$  to  $120^\circ\text{C}$  was due to evaporation of surface adsorbed water because samples adsorbed water during its curing at room temperature. The second endothermic effect was in temperature range from  $120^\circ\text{C}$  to  $400^\circ\text{C}$ , is attributed to the dehydration of C-S-H and calcium aluminoferrite.

#### **(a). NanoSiO<sub>2</sub>**

Total weight loss for cement between  $25^\circ\text{C}$  to  $120^\circ\text{C}$  for the NanoSiO<sub>2</sub> was 1.33% as summarized in Table 1. When the temperature changed from  $120^\circ\text{C}$  to  $400^\circ\text{C}$ , the weight loss of the NanoSiO<sub>2</sub> increased to 3.0% as summarized in Table 1. For temperature range between  $400^\circ\text{C}$  to  $600^\circ\text{C}$ , the weight loss for NanoSiO<sub>2</sub> was 0.85% as summarized in Table 1. When the temperature changed from  $600^\circ\text{C}$  to  $800^\circ\text{C}$ , the weight loss for was 5.13% for the NanoSiO<sub>2</sub> as summarized in Table 1. Total weight loss for the NanoSiO<sub>2</sub> was 10.31% also shown in Figure 2.

#### **(b). Smart Cement Powder**

Total weight loss for the cement powder between  $25^\circ\text{C}$  to  $120^\circ\text{C}$  was 0.56% as summarized in Table 1. When the temperature changed from  $120^\circ\text{C}$  to  $400^\circ\text{C}$ , the weight loss of the cement increased to 0.66%. For temperature range between  $400^\circ\text{C}$  to  $600^\circ\text{C}$ , the total weight loss for cement was 1.44%. When the temperature changed from  $600^\circ\text{C}$  to  $800^\circ\text{C}$ , the weight loss for cement increased to 3.44% as summarized in Table 1. Total weight loss for the cement was 6.10%.

#### **(c). Smart Cement and 1% NanoSiO<sub>2</sub>**

The weight loss for cement modified with 1% NanoSiO<sub>2</sub> between  $25^\circ\text{C}$  to  $120^\circ\text{C}$  was 0.07% as summarized in Table 1. The NanoSiO<sub>2</sub> addition strongly modified the free water dehydration ( $25^\circ\text{C}$  -  $120^\circ\text{C}$ ). When the temperature changed from  $120^\circ\text{C}$  to  $400^\circ\text{C}$ , the weight loss was 0.33%. The weight loss in the temperature between  $400^\circ\text{C}$  to  $600^\circ\text{C}$ , indicates the decomposition of  $\text{Ca}(\text{OH})_2$  formed during hydration.

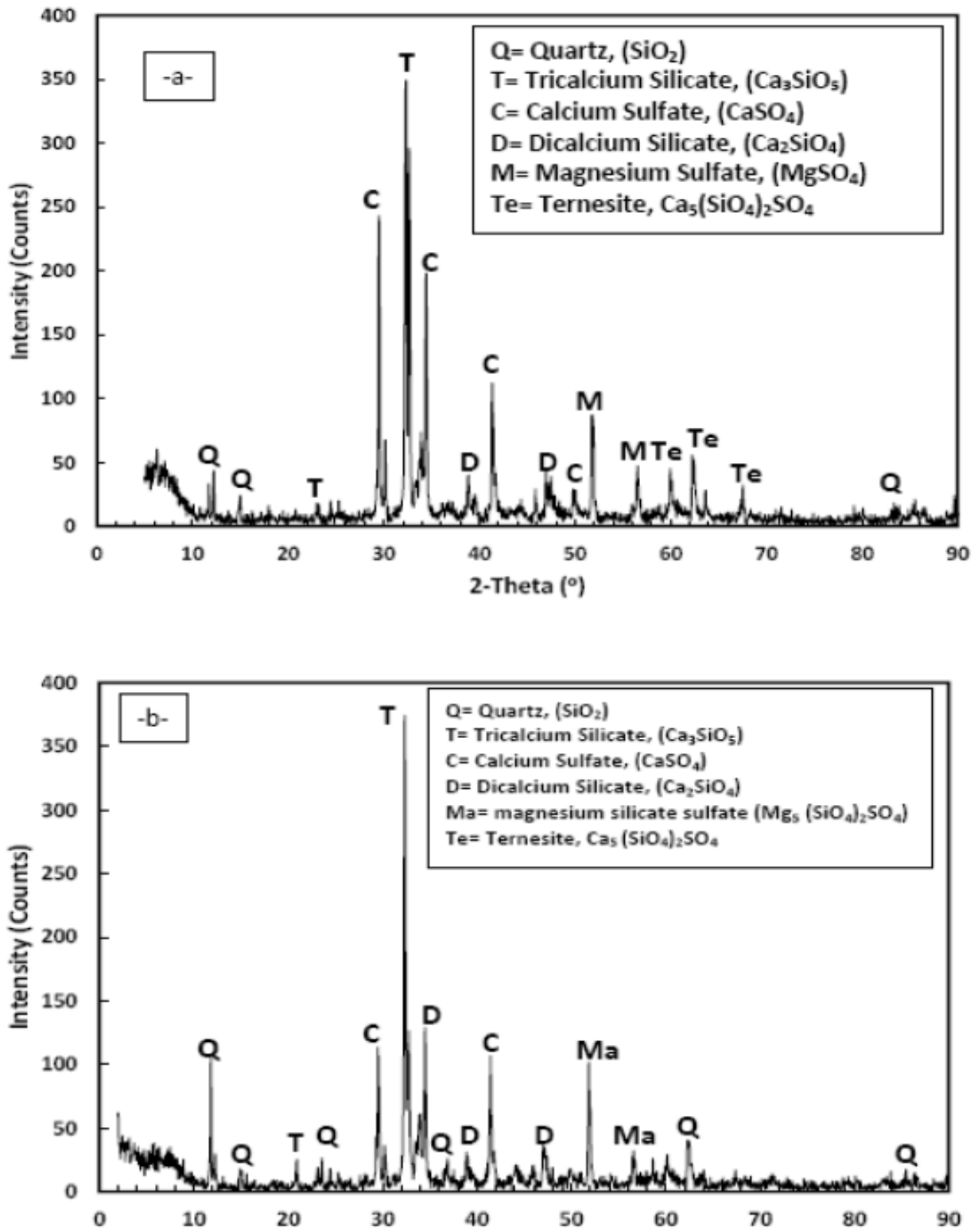
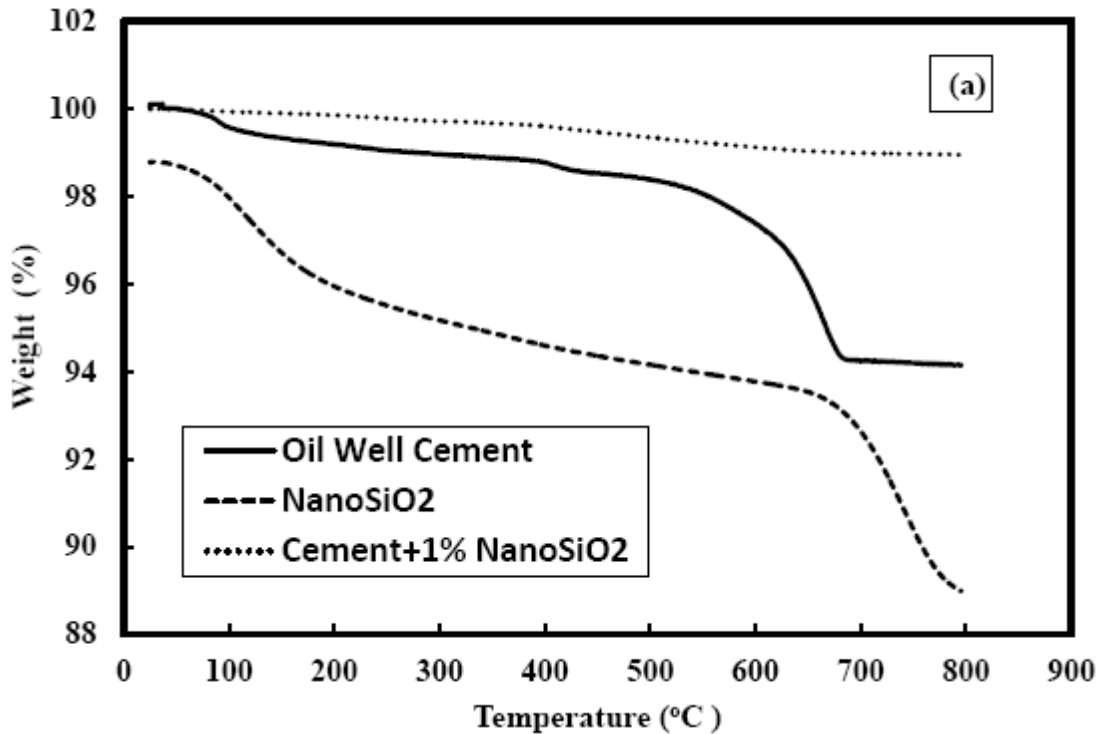


Figure 1. XRD Patterns (a) Oil well cement (b) Oil well cement+1% NanoSiO<sub>2</sub>

For temperature range between 400°C to 600°C, the weight loss was only 0.49%. When the temperature changed from 600°C to 800°C, the weight loss was 0.16%, a 95% reduction compared to the cement in the temperatures range of 600°C to 800°C as summarized in Table 1. Finally, an endothermic reaction at 800°C indicates the decarbonation of calcium carbonate in the hydrated cement compound. The total weight loss was only 1.05%, very small in the cement modified with 1% NanoSiO<sub>2</sub> indicative of the NanoSiO<sub>2</sub> interaction with the cement paste.

**Table 1. TGA results on the NanoSiO<sub>2</sub> and the oil well cement with and without 1% NanoSiO<sub>2</sub>**

Temperature Range \ Type of Sample	Weight Loss (%)				
	25-120°C	120-400°C	400-600°C	600-800°C	Total (%)
NanoSiO <sub>2</sub>	1.33	3.0	0.85	5.13	10.31
Smart cement powder	0.56	0.66	1.44	3.44	6.10
Smart cement + 1% NanoSiO <sub>2</sub>	0.07	0.33	0.49	0.16	1.05



**Figure 2. Thermogravimetric analyses (TGA) weight loss results on the smart cement and NanoSiO<sub>2</sub> and a Mixture.**

**Density and Initial Resistivity**

**(a). Smart Cement**

The average density of the smart cement with less than 0.1% carbon fiber was 1.975 g/cc (16.47 ppg). The initial electrical resistivity ( $\rho_o$ ) of the smart cement mix with a w/c ratio of 0.38 was 1.06  $\Omega$ m.

**(b). Smart Cement with 0.5% NanoSiO<sub>2</sub>**

The average density of the smart cement with 0.5% NanoSiO<sub>2</sub> was 1.977 g/cc (16.49 ppg), 0.1% increase in density. The initial electrical resistivity ( $\rho_o$ ) of smart cement with 0.5% NanoSiO<sub>2</sub> was 1.20  $\Omega$ m, a 13% increase in the electrical resistivity as shown in Figure 3. The resistivity was more sensitive to the NanoSiO<sub>2</sub> addition than the density.

**(c). Smart Cement with 1% NanoSiO<sub>2</sub>**

The average density of the smart cement with 1% NanoSiO<sub>2</sub> was 1.982 g/cc (16.53 ppg), about 0.4% increase in density. The initial electrical resistivity ( $\rho_o$ ) of smart cement with 1.0% NanoSiO<sub>2</sub> was 1.39  $\Omega$ m, a 31% increase in the electrical resistivity as shown in Figure 3. The resistivity was more sensitive to the 1% NanoSiO<sub>2</sub> addition than the density.

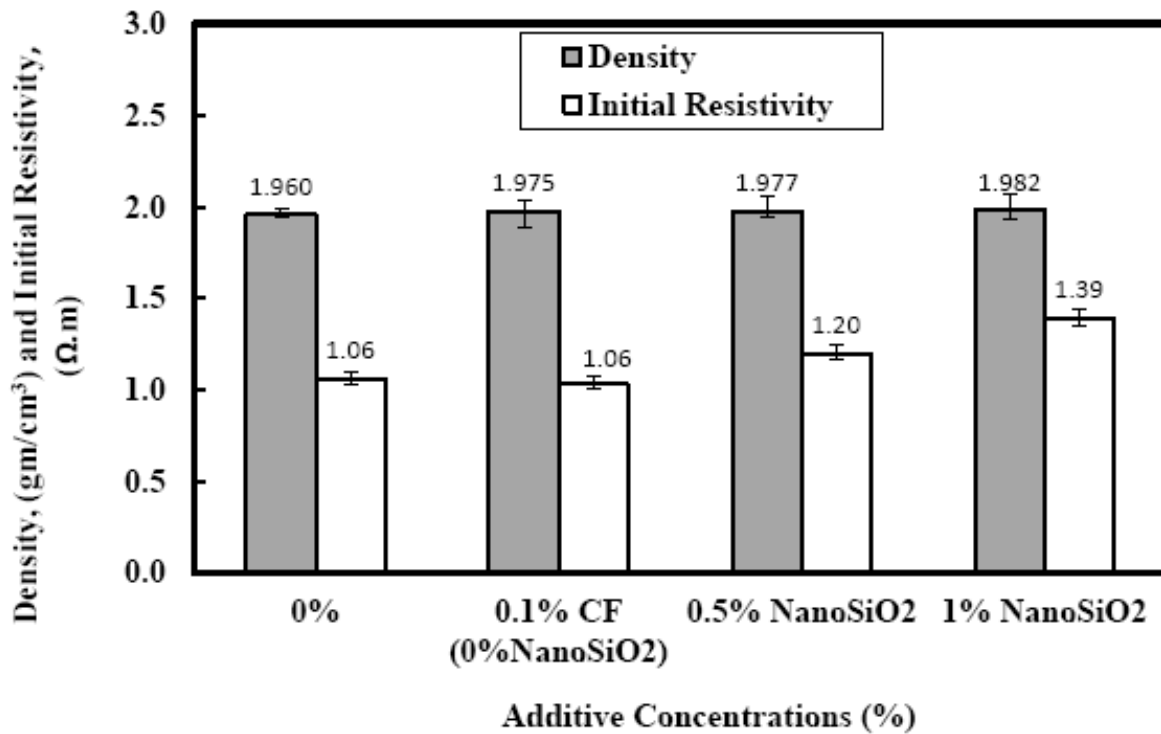


**Figure 3. Effect of 1% NanoSiO<sub>2</sub> on the Density and Initial Resistivity of Smart Cement**

**Curing**

Change in the electrical resistivity with time and the minimum resistivity quantifies the formation of solid hydration products, which leads to a decrease in the porosity which influences the cement strength development.

### Vipulanandan curing model

Based on experimental results, model proposed by Vipulanandan was used to predict the electrical resistivity of smart cement during hydration up to 28 days of curing as shown in Figure 5. The curing model is defined as follows:

$$\frac{1}{\rho} = \left(\frac{1}{\rho_{min}}\right) \left( \frac{\left(\frac{t+t_0}{t_{min}+t_0}\right)}{q_1 + (1-p_1-q_1) \left(\frac{t+t_0}{t_{min}+t_0}\right) + p_1 \left(\frac{t+t_0}{t_{min}+t_0}\right)^{\frac{q_1+p_1}{p_1}}} \right) \quad (4)$$

where  $\rho$ : electrical resistivity ( $\Omega$ -m);  $\rho_{min}$ : minimum electrical resistivity ( $\Omega$ -m);  $t_{min}$ : time corresponding minimum electrical resistivity ( $\rho_{min}$ );  $p_1$ ,  $t_0$ , and  $q_1$  are model parameters; and  $t$ : time (minutes).

#### (a). Smart Cement

The minimum resistivity ( $\rho_{min}$ ) of smart cement was 0.85  $\Omega$ m and the time to reach the minimum resistivity ( $t_{min}$ ) was 99 minutes as summarized in Table 2. The resistivity after 24 hours was 3.90  $\Omega$ m, representing a change of about 268 % in 24 hours as shown in Figure 4 (a). The resistivity index ( $RI_{24hr}$ ) for smart cement were 364%, represents the maximum resistivity change in 24 hours as summarized in Table 2. The resistivity after 7 days and 28 days were 7.7  $\Omega$ m and 35.7  $\Omega$ m respectively and also shown in Figure 4 (b) and (c). These observed trends clearly indicate the sensitivity of resistivity to the changes occurring in the curing of cement as summarized in Table 2.

#### (b). Smart Cement with 0.5% NanoSiO<sub>2</sub>

The minimum resistivity ( $\rho_{min}$ ) of smart cement with 0.5% NanoSiO<sub>2</sub> was 0.95  $\Omega$ -m, which was 12% higher compared to the smart cement minimum electrical resistivity. The time to reach the minimum resistivity ( $t_{min}$ ) was 110 minutes as summarized in Table 2 and it was 11% higher than the smart cement. The resistivity after 24 hours was 4.16  $\Omega$ m, representing a change of about 289 % in 24 hours as shown in Figure 4 (a). The resistivity index ( $RI_{24hr}$ ) for smart cement with 0.5% NanoSiO<sub>2</sub> was 338% as summarized in Table 2. The resistivity after 7 days and 28 days were 8.0  $\Omega$ m and 27.8  $\Omega$ m respectively and also shown in Figures 4(b) and 4(c). Change in  $RI_{24hr}$  decreased with the 0.5% NanoSiO<sub>2</sub> content. These observed trends clearly indicate the sensitivity of resistivity to the changes occurring in the curing of cement as summarized in Table 2.

#### (c). Smart Cement with 1% NanoSiO<sub>2</sub>

The minimum resistivity ( $\rho_{min}$ ) of smart cement with 1% of NanoSiO<sub>2</sub> 1.11  $\Omega$ -m, which was about 30% higher compared to the smart cement minimum electrical resistivity. The time to reach the minimum resistivity ( $t_{min}$ ) was 122 minutes as summarized in Table 2 which was about 23% higher than the smart cement. The resistivity after 24 hours was 4.76  $\Omega$ m, representing a change of about 242 % in 24 hours as shown in Figure 4 (a). The resistivity after 7 days and 28 days were 8.7  $\Omega$ m and 20.6  $\Omega$ m respectively and also shown in Figures 4(b) and 4(c). The resistivity index ( $RI_{24hr}$ ) for smart cement with 1% of NanoSiO<sub>2</sub> was 328% as summarized in Table

2. Change in  $RI_{24hr}$  decreased with 1%  $NanoSiO_2$  content. These observed trends clearly indicate the sensitivity of resistivity to the changes occurring in the curing of cement as summarized in Table 2.

**Table 2. Curing Bulk Resistivity Parameters for the Smart Cement with  $NanoSiO_2$**

NanoSiO <sub>2</sub> (%)	Initial resistivity, $\rho_o$ ( $\Omega$ -m)	$\rho_{min}$ ( $\Omega$ -m)	$t_{min}$ (min)	$\rho_{24hr}$ ( $\Omega$ -m)	$\rho_{7\text{ days}}$ ( $\Omega$ -m)	$RI_{24\text{ hr}}$ (%)	$RI_{7\text{ days}}$ (%)
0	1.06 ± 0.02	0.85 ± 0.02	99 ± 5	3.90 ± 0.04	7.7 ± 0.5	364	806
0.5	1.20 ± 0.03	0.95 ± 0.05	110 ± 7	4.16 ± 0.01	8.0 ± 0.4	338	708
1	1.39 ± 0.03	1.11 ± 0.03	122 ± 4	4.76 ± 0.03	8.7 ± 0.8	328	684

Vipulanandan curing model (Eqn. (4)) was used to predict the resistivity changes with the curing time for 1 day, 7 days and 28 days of curing as shown in Figure 4. The model predicted the experimental results very well. The model parameters  $p_1$ ,  $q_1$  and the ratio  $q_1/p_1$  were all sensitive to the amount of  $NanoSiO_2$  added to the cement. Also the parameters  $t_{min}$  and  $\rho_{min}$  can be used as quality control indices and were related to the  $NanoSiO_2$  content as follows:

$$t_{min} = 23 * (NanoSiO_2(\%)) + 99 \quad R^2=0.99 \quad (5)$$

$$\rho_{min} = 0.85 + 0.26 * (NanoSiO_2(\%)) \quad R^2=0.98 \quad (6)$$

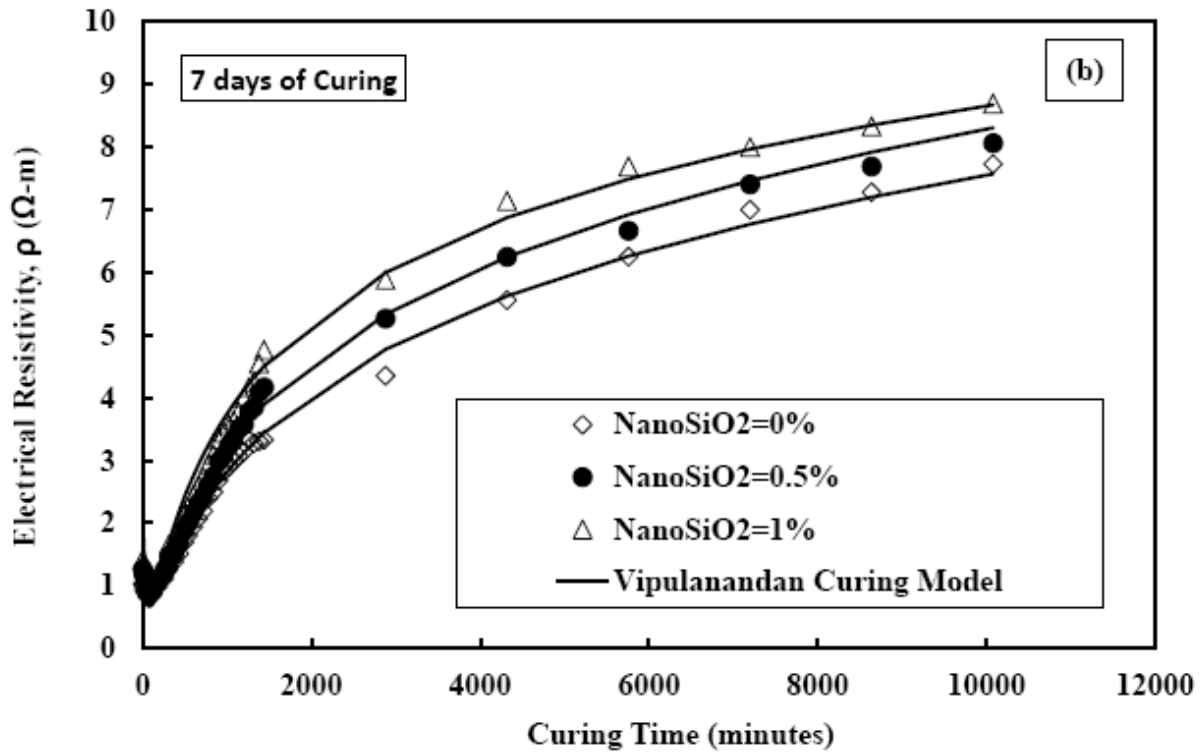
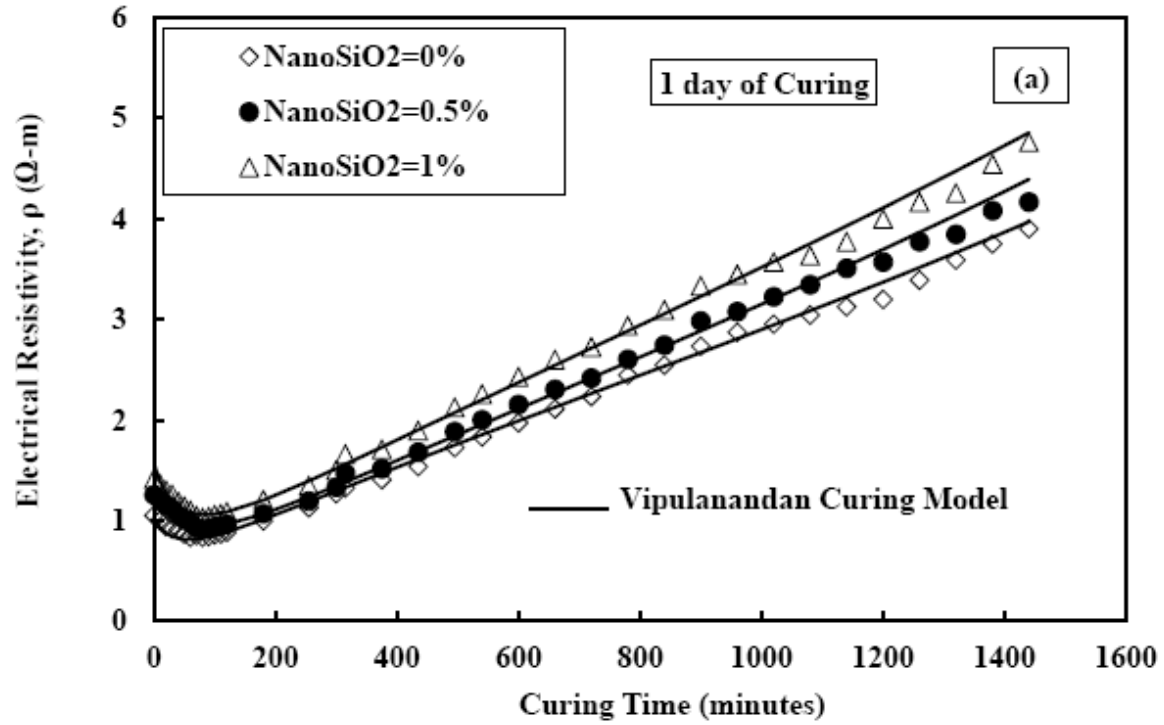
Hence the electrical resistivity parameters were linearly related to the  $NanoSiO_2$  content.

### Compressive Stress-Strain Behavior

Based on the experimental results Vipulanandan p-q stress-strain model (Eqn. (7)) was used to predict the compressive stress-strain relationship for smart cement with and without  $NanoSiO_2$  and the relationship is as follows:

$$\sigma_c = \frac{\frac{\epsilon_c}{\epsilon_{cf}} * \sigma_{cf}}{q_o + (1 - p_o - q_o) \frac{\epsilon_c}{\epsilon_{cf}} + p \left( \frac{\epsilon_c}{\epsilon_{cf}} \right)^{\frac{(p_o + q_o)}{p_o}}} \quad (7)$$

where:  $\sigma_c$  is compressive stress and  $\epsilon_c$  compressive strain;  $\sigma_{cf}$  and  $\epsilon_{cf}$  are compressive strength and corresponding strain as summarized in Table 7.3. The model parameters  $p_o$ , and  $q_o$  are also summarized in Table 3. Model parameters  $p_o$  and  $q_o$  increased with curing time based on the  $NanoSiO_2$  content. The compressive stress-strain relationships for the cement with and without  $NanoSiO_2$  are shown in Figure 5.



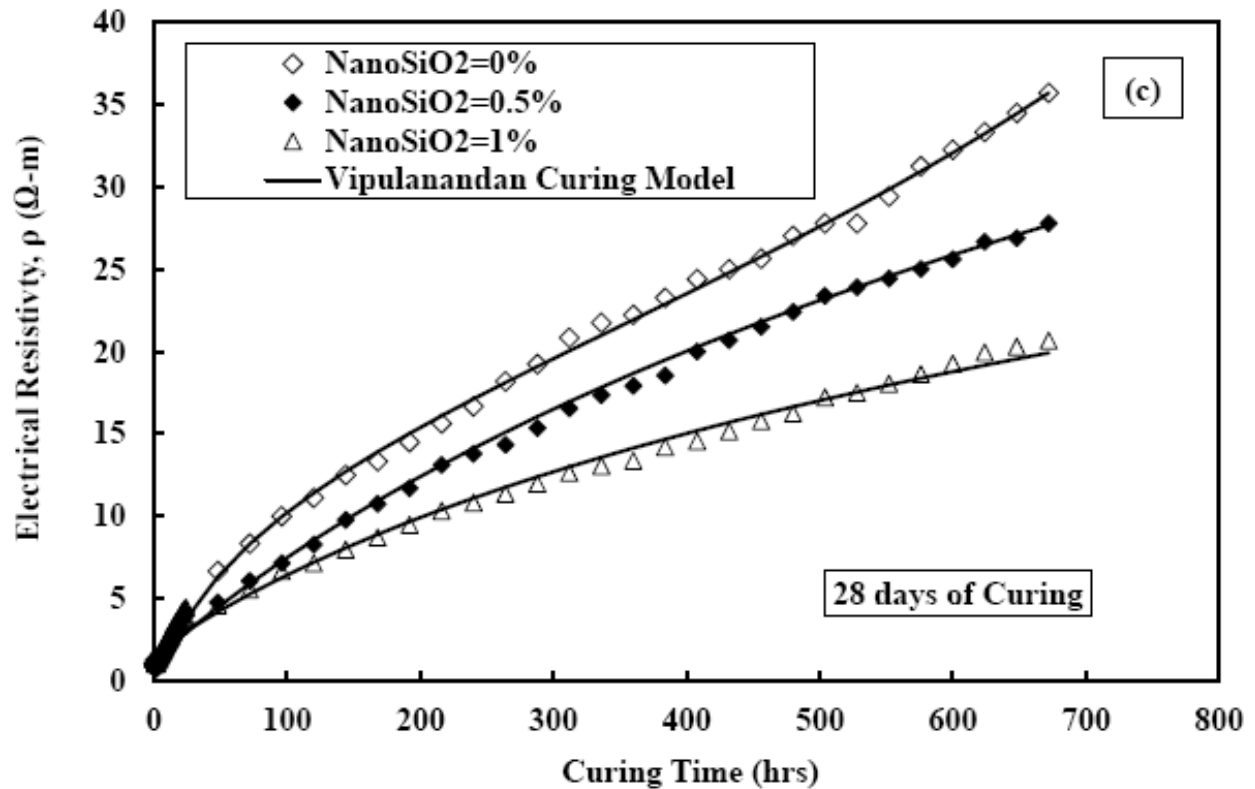


**Figure 4. Bulk electrical resistivity development of smart cement with various amount of NanoSiO<sub>2</sub> (a) 1 day (b) 7 days and (c) 28 days**

**(a). 1 day Curing**

**(i). Smart Cement**

The compressive strengths ( $\sigma_{cf}$ ) of the smart cement after 1 day of curing were 10.9 MPa, as shown in Figure 5. The failure strain was 0.30% and the initial modulus was 10,100 MPa as summarized in Table 3. The model parameters  $q_0$  and  $p_0$  were 0.36 and 0.034 respectively. The parameter  $q_0$  represents the nonlinearity up to peak stress, and the smart cement had the highest nonlinearity, lowest value of parameter  $q_0$  as shown in Figure 7.5. The coefficient of determination ( $R^2$ ) was 0.99 and the root-mean-square error (RMSE) was 0.128 MPa as summarized in Table 3.

**(ii). Smart Cement with 0.5% NanoSiO<sub>2</sub>**

The compressive strengths ( $\sigma_{cf}$ ) of the smart cement with 0.5% NanoSiO<sub>2</sub> after 1 day of curing were 11.6 MPa, 6.4% higher than the smart cement without NanoSiO<sub>2</sub> as shown in Figure 5. The failure strain was 0.25% and the initial modulus was 10,800 MPa as summarized in Table 3. Addition of 0.5% NanoSiO<sub>2</sub> to the smart cement reduced the failure strain and increased the modulus compared to the smart cement without NanoSiO<sub>2</sub>. The model parameters  $q_0$  and  $p_0$  were 0.43 and 0.061 respectively. The parameter  $q_0$  represents the nonlinearity up to peak stress, and was higher than the smart cement without NanoSiO<sub>2</sub> as shown in Figure 5. The coefficient of determination ( $R^2$ ) was 0.99 and the root-mean-square error (RMSE) was 0.095 MPa as summarized in Table 3.

**(iii). Smart Cement with 1% NanoSiO<sub>2</sub>**

The compressive strengths ( $\sigma_{cf}$ ) of the smart cement with 1% NanoSiO<sub>2</sub> after 1 day of curing were 12.4 MPa, 13.8% higher than the smart cement without NanoSiO<sub>2</sub> as shown in Figure 5. The failure strain was 0.22% and the initial modulus was 11,000 MPa as summarized in Table 3. Addition of 1% NanoSiO<sub>2</sub> to the smart cement reduced the failure strain and increased the modulus compared to the smart cement without NanoSiO<sub>2</sub>. The model parameters  $q_0$  and  $p_0$  were 0.53 and 0.094 respectively. The parameter  $q_0$  represents the nonlinearity up to peak stress, and was higher than the smart cement without NanoSiO<sub>2</sub> as shown in Figure 5. The coefficient of determination ( $R^2$ ) was 0.99 and the root-mean-square error (RMSE) was 0.244 MPa as summarized in Table 3.

**Table 3. Compressive stress-strain model parameters for the NanoSiO<sub>2</sub> modified smart cement after one day of curing**

NanoSiO <sub>2</sub> (%)	Curing Time (day)	$\sigma_{cf}$ (MPa)	$\epsilon_{cf}$ (%)	Ei (MPa)	$p_0$	$q_0$	RMSE (MPa)	R <sup>2</sup>
0	1	10.9 ± 2	0.30 ± 0.02	10,100	0.034 ± 0.03	0.36 ± 0.02	0.128	0.99
0.5	1	11.6 ± 3	0.25 ± 0.02	10,800	0.061 ± 0.03	0.43 ± 0.02	0.095	0.99
1	1	12.4 ± 2	0.22 ± 0.02	11,000	0.094 ± 0.02	0.53 ± 0.03	0.244	0.99

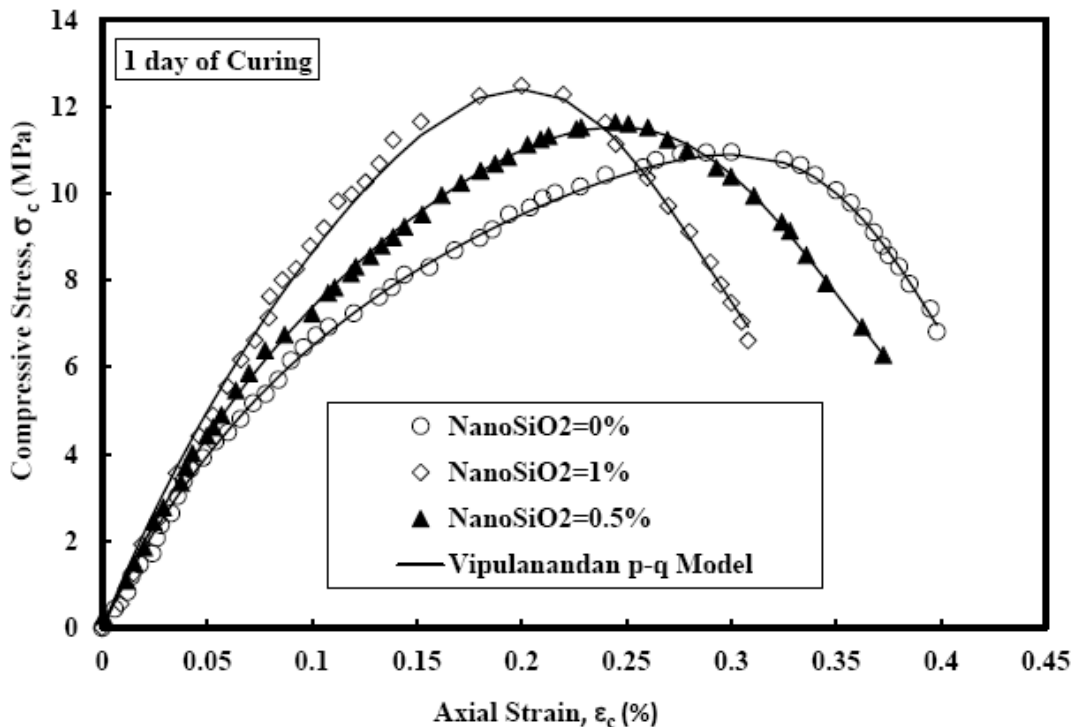


**Figure 5. Compressive Stress- Strain Relationship for Modified Smart Cement with**

**28 Days of Curing**

**(a). Smart Cement**

The compressive strengths ( $\sigma_{cf}$ ) of the smart cement after 28 days of curing were 19.3 MPa, as shown in Figure 6. The failure strain was 0.22% and the initial modulus was 12,500 MPa as summarized in Table 4. The model parameters  $q_0$  and  $p_0$  were 0.70 and 0.160 respectively. The parameter  $q_0$  represents the nonlinearity up to peak stress, and the smart cement had the highest linearity, highest value of parameter  $q_0$  as shown in Figure 6. The coefficient of determination ( $R^2$ ) was 0.99 and the root-mean-square error (RMSE) was 0.110 MPa as summarized in Table 4.

**(b). Smart Cement with 0.5% NanoSiO<sub>2</sub>**

The compressive strengths ( $\sigma_{cf}$ ) of the smart cement with 0.5% NanoSiO<sub>2</sub> after 28 days of curing were 22.3 MPa, 15.5% higher than the smart cement without NanoSiO<sub>2</sub> as shown in Figure 6. The failure strain was 0.20% and the initial modulus was 18,600 MPa as summarized in Table 4. Addition of 0.5% NanoSiO<sub>2</sub> to the smart cement reduced the failure strain and increased the modulus compared to the smart cement without NanoSiO<sub>2</sub>. The model parameters  $q_0$  and  $p_0$  were 0.60 and 0.092 respectively. The parameter  $q_0$  represents the nonlinearity up to peak stress, and was lower than the smart cement without NanoSiO<sub>2</sub> as shown in Figure 6. The coefficient of determination ( $R^2$ ) was 0.99 and the root-mean-square error (RMSE) was 0.085 MPa as summarized in Table 4.

**(c). Smart Cement with 1% NanoSiO<sub>2</sub>**

The compressive strengths ( $\sigma_{cf}$ ) of the smart cement with 1% NanoSiO<sub>2</sub> after 28 days of curing were 27.5 MPa, 42.5% higher than the smart cement without NanoSiO<sub>2</sub> as shown in Figure 6. The failure strain was 0.19% and the initial modulus was 25,400 MPa as summarized in Table 4. Addition of 1% NanoSiO<sub>2</sub> to the smart cement reduced the failure strain and doubled the modulus, 100% increase compared to the smart cement without NanoSiO<sub>2</sub>. The model parameters  $q_0$  and  $p_0$  were 0.57 and 0.100 respectively. The parameter  $q_0$  represents the nonlinearity up to peak stress, and was lower than the smart cement without NanoSiO<sub>2</sub> as shown in Figure 5. The coefficient of determination ( $R^2$ ) was 0.99 and the root-mean-square error (RMSE) was 0.150 MPa as summarized in Table 4.

**Table 4. Compressive stress-strain model parameters for the NanoSiO<sub>2</sub> modified smart cement after 28 days of curing**

NanoSiO <sub>2</sub> (%)	Curing Time (day)	$\sigma_{cf}$ (MPa)	$\epsilon_{cf}$ (%)	Ei (MPa)	$p_0$	$q_0$	RMSE (MPa)	R <sup>2</sup>
0	28	19.3 ± 1	0.22 ± 0.02	12,500	0.160 ± 0.01	0.70 ± 0.03	0.110	0.99
0.5	28	22.3 ± 2	0.20 ± 0.02	18,600	0.092 ± 0.02	0.60 ± 0.02	0.085	0.99
1.0	28	27.5 ± 3	0.19 ± 0.02	25,400	0.100 ± 0.01	0.57 ± 0.01	0.150	0.99

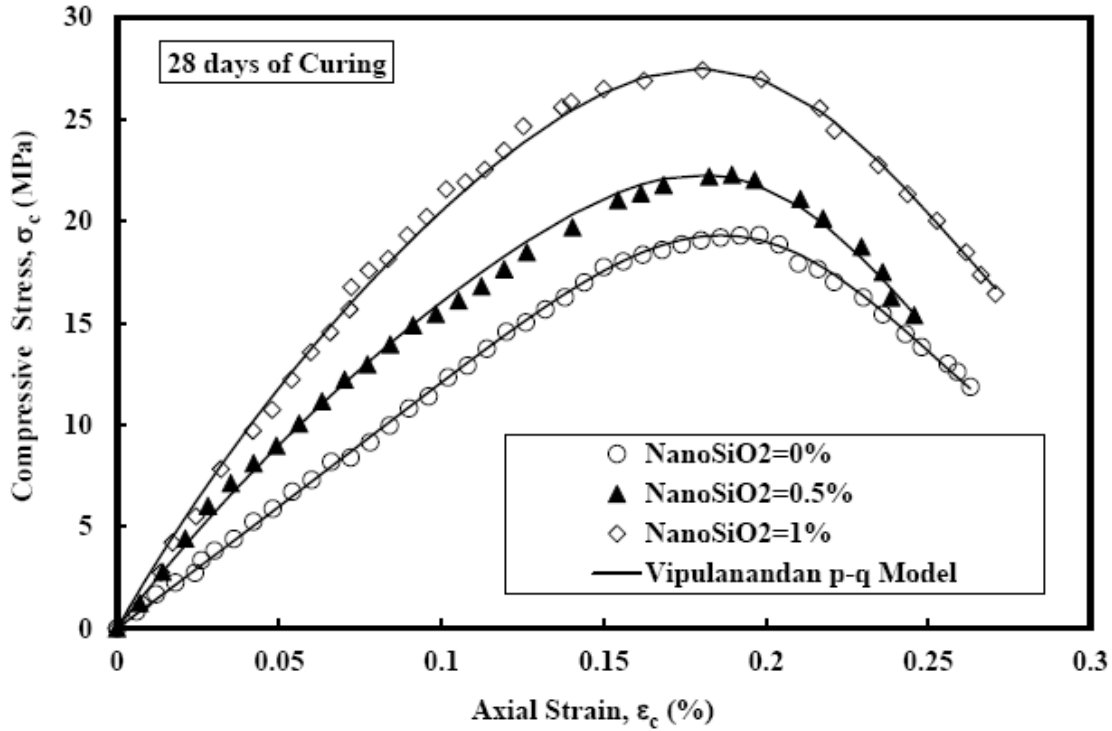


**Figure 6. Compressive Stress- Strain Relationship of Modified Smart Cement with 28 days of Curing**

**Compressive Piezoresistivity Behavior**

Based on experimental results, Vipulanandan p-q piezoresistivity model was developed to predict the change in electrical resistivity of the smart cement during with applied compressive stress for 1 day, 7 days and 28 days of curing. The Vipulanandan Piezoresistive model is defined as follows:

$$\sigma_c = \frac{\frac{x}{x_f} * \sigma_{cf}}{q_2 + (1 - p_2 - q_2) \frac{x}{x_f} + p_2 \left(\frac{x}{x_f}\right)^{\frac{p_2}{p_2 - q_2}}} \tag{8}$$

where  $\sigma_c$  is the stress (MPa);  $\sigma_{cf}$  is the compressive strength at failure (MPa);  $x = \left(\frac{\Delta\rho}{\rho_o}\right) * 100$  is the Percentage piezoresistive axial strain due to the applied stress;  $x_f = \left(\frac{\Delta\rho}{\rho_o}\right)_f * 100$  : Percentage piezoresistive axial strain at failure;  $\Delta\rho$ : change in electrical resistivity;  $\rho_o$  : initial electrical resistivity ( $\sigma = 0$  MPa) and  $p_2$  and  $q_2$  are the piezoresistive model parameters.

**1 day of Curing**

**(a). Smart Cement**

The piezoresistive axial strain of the smart cement at failure  $\left(\frac{\Delta\rho}{\rho_o}\right)_f$  after 1 day of curing was 520%, as summarized in Table 5 and shown in Figure 7. The compressive axial failure strain

was 0.30%, so the piezoresistive axial strain has been increased by 1,733 times (173,300%) making the smart cement to be highly sensing. The model parameters  $q_2$  and  $p_2$  were 0.29 and 0.16 respectively. The coefficient of determination ( $R^2$ ) was 0.99 and the root-mean-square error (RMSE) was 0.054 MPa as summarized in Table 5.

**(b). Smart Cement with 0.5% NanoSiO<sub>2</sub>**

The piezoresistive axial strain of the smart cement with 0.5% NanoSiO<sub>2</sub> at failure  $\left(\frac{\Delta\rho}{\rho_o}\right)_f$  after 1 day of curing was 495%, as summarized in Table 5 and shown in Figure 7. Addition of 0.5% NanoSiO<sub>2</sub> reduced the piezoresistive axial strain of smart cement by 4.8%. The compressive axial failure strain was 0.25%, so the piezoresistive axial strain has been increased by 1,980 times (198,000%) making the smart cement to be highly sensing. The model parameters  $q_2$  and  $p_2$  were 0.19 and 0.17 respectively. The coefficient of determination ( $R^2$ ) was 0.99 and the root-mean-square error (RMSE) was 0.019 MPa as summarized in Table 5.

**(c). Smart Cement with 1% NanoSiO<sub>2</sub>**

The piezoresistive axial strain of the smart cement with 1% NanoSiO<sub>2</sub> at failure  $\left(\frac{\Delta\rho}{\rho_o}\right)_f$  after 1 day of curing was 428%, as summarized in Table 5 and shown in Figure 7. Addition of 1% NanoSiO<sub>2</sub> reduced the piezoresistive axial strain of smart cement by 17.7%. The compressive axial failure strain was 0.22%, so the piezoresistive axial strain has been increased by 1,945 times (194,500%) making the smart cement to be highly sensing. The model parameters  $q_2$  and  $p_2$  were 0.30 and 0.19 respectively. The coefficient of determination ( $R^2$ ) was 0.99 and the root-mean-square error (RMSE) was 0.010 MPa as summarized in Table 5.

**Table 5. Piezoresistive Axial Strain at failure and Strength of the Smart Cement without and with NanoSiO<sub>2</sub> After one Day of Curing**

Material	NanoSiO <sub>2</sub> (%)	Curing Time (day)	$\left(\frac{\Delta\rho}{\rho_o}\right)_f$ (%)	$\sigma_{cf}$ (MPa)	$p_2$	$q_2$	RMSE (MPa)	$R^2$
Smart Cement	0%	1	520 ± 10	10.9 ± 3	0.16 ± 0.02	0.29 ± 0.02	0.054	0.99
Smart Cement	0.5%	1	495 ± 8	11.6 ± 5	0.17 ± 0.06	0.19 ± 0.02	0.019	0.99
Smart Cement	1%	1	428 ± 10	12.4 ± 2	0.19 ± 0.02	0.30 ± 0.04	0.010	0.99

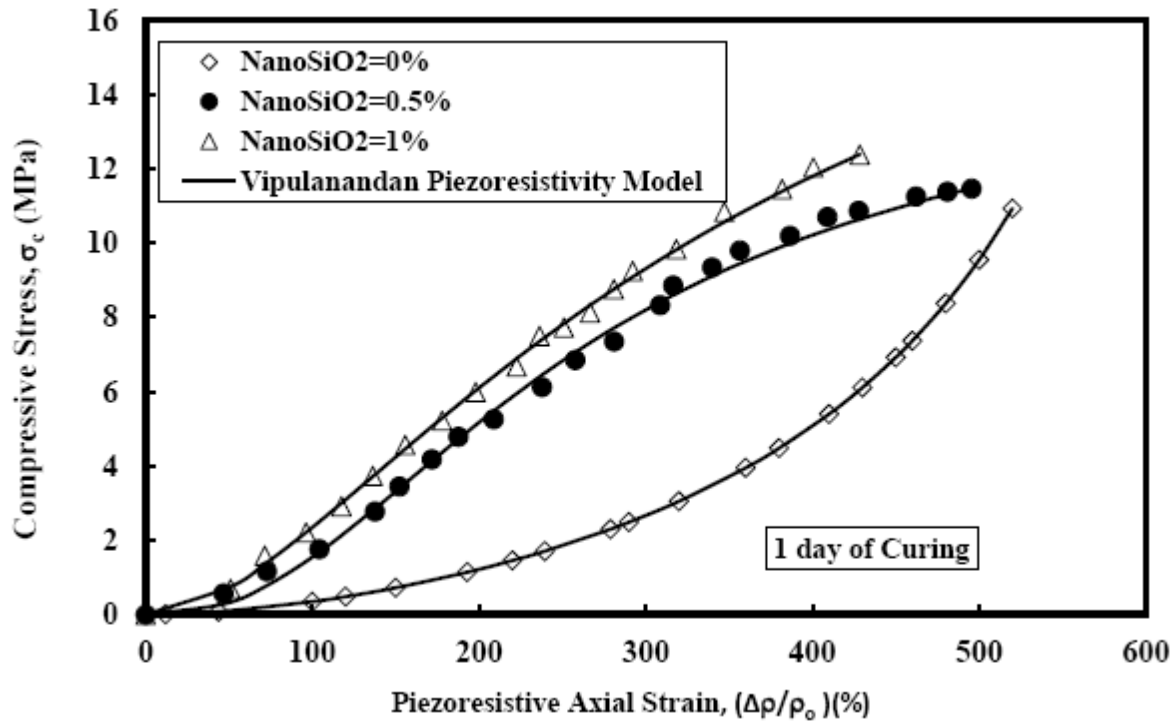


**Figure 7. Piezoresistive behavior of smart cement with various amounts of NanoSiO<sub>2</sub> After 1 Day of Curing**  
7 days of Curing

**(a). Smart Cement**

The piezoresistive axial strain of the smart cement at failure  $\left(\frac{\Delta\rho}{\rho_o}\right)_f$  after 7 days of curing was 460%, as summarized in Table 6 and shown in Figure 8. Compressive piezoresistive axial strain at failure reduced by 11.5% after 7 days of curing. The model parameters  $q_2$  and  $p_2$  were 0.04 and 0.11 respectively. The coefficient of determination ( $R^2$ ) was 0.99 and the root-mean-square error (RMSE) was 0.017 MPa as summarized in Table 6.

**(b). Smart Cement with 0.5% NanoSiO<sub>2</sub>**

The piezoresistive axial strain of the smart cement with 0.5% NanoSiO<sub>2</sub> at failure  $\left(\frac{\Delta\rho}{\rho_o}\right)_f$  after 7 days of curing was 409%, as summarized in Table 6 and shown in Figure 8. Compressive piezoresistive axial strain at failure reduced by 17.3% after 7 days of curing and the percentage reduction was higher than the smart cement without NanoSiO<sub>2</sub>. The model parameters  $q_2$  and  $p_2$  were 0.18 and 0.10 respectively. The coefficient of determination ( $R^2$ ) was 0.99 and the root-mean-square error (RMSE) was 0.003 MPa as summarized in Table 6.

**(c). Smart Cement with 1% NanoSiO<sub>2</sub>**

The piezoresistive axial strain of the smart cement with 1% NanoSiO<sub>2</sub> at failure  $\left(\frac{\Delta\rho}{\rho_o}\right)_f$  after 7 days of curing was 365%, as summarized in Table 6 and shown in Figure 8. Compressive piezoresistive axial strain at failure reduced by 14.7% after 7 days of curing and the percentage

reduction was higher than the smart cement without NanoSiO<sub>2</sub>. The model parameters q<sub>2</sub> and p<sub>2</sub> were 0.33 and 0.18 respectively. The coefficient of determination (R<sup>2</sup>) was 0.99 and the root-mean-square error (RMSE) was 0.018 MPa as summarized in Table 6.

**Table 6. Piezoresistive axial strain at failure and Strength of the Smart Cement without and with NanoSiO<sub>2</sub> after 7 Days of Curing**

Material	NanoSiO <sub>2</sub> (%)	Curing Time (day)	$\left(\frac{\Delta\rho}{\rho_o}\right)_f$ (%)	$\sigma_{cr}$ (MPa)	p <sub>2</sub>	q <sub>2</sub>	RMSE (MPa)	R <sup>2</sup>
Smart Cement	0%	7	460 ± 14	16.0 ± 3	0.11 ± 0.04	0.04 ± 0.05	0.017	0.99
	0.5%	7	409 ± 9	18.1 ± 2	0.10 ± 0.02	0.18 ± 0.03	0.003	0.99
	1%	7	365 ± 12	21.2 ± 4	0.18 ± 0.03	0.33 ± 0.02	0.018	0.99

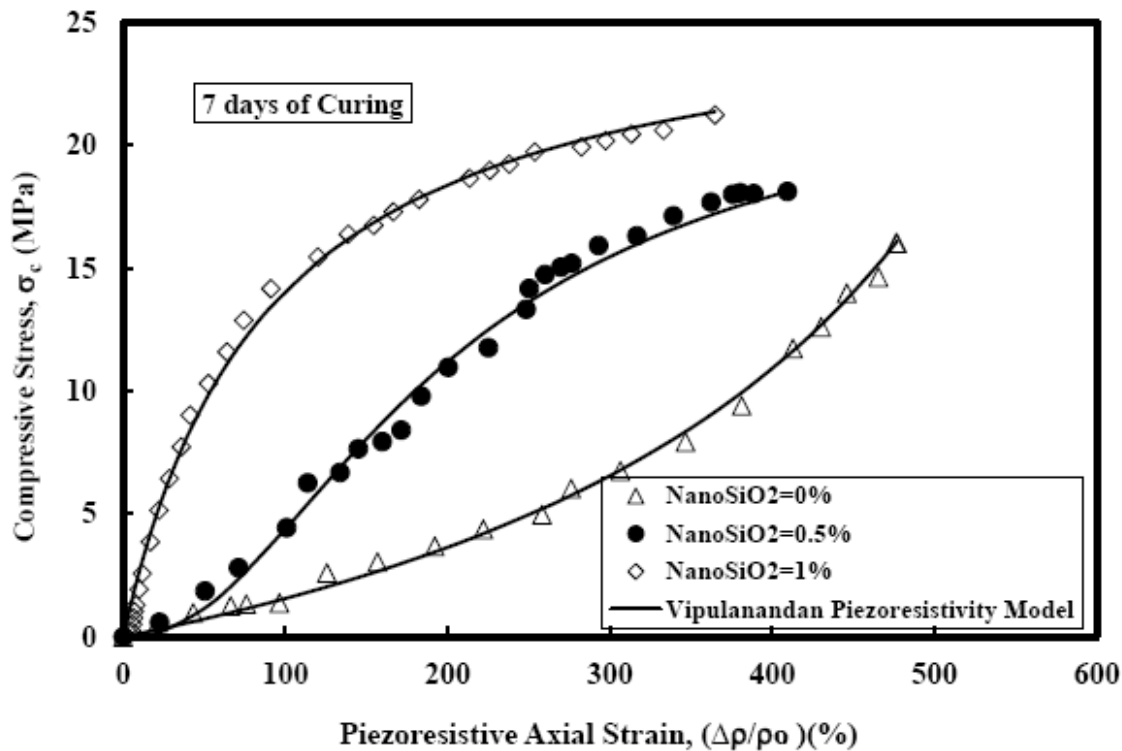


**Figure 8. Piezoresistive behavior of smart cement with various amount of NanoSiO<sub>2</sub> after 7 days of curing**

**28 days of Curing**  
**(a). Smart Cement**

The piezoresistive axial strain of the smart cement at failure  $\left(\frac{\Delta\rho}{\rho_o}\right)_f$  after 28 days of curing was 400%, as summarized in Table 7 and shown in Figure 9. Compressive piezoresistive axial strain at failure reduced by 23% after 28 days of curing. The compressive axial failure strain was 0.22%, so the piezoresistive axial strain has been increased by 1,818 times (181,800%) making the

smart cement to be highly sensing. The model parameters  $q_2$  and  $p_2$  were 0.05 and 0.03 respectively. The coefficient of determination ( $R^2$ ) was 0.99 and the root-mean-square error (RMSE) was 0.022 MPa as summarized in Table 7.

**(b). Smart Cement with 0.5% NanoSiO<sub>2</sub>**

The piezoresistive axial strain of the smart cement with 0.5% NanoSiO<sub>2</sub> at failure  $\left(\frac{\Delta\rho}{\rho_o}\right)_f$  after 28 days of curing was 334%, as summarized in Table 7 and shown in Figure 9. Compressive piezoresistive axial strain at failure reduced by 32.5% after 28 days of curing and the percentage reduction was higher than the smart cement without NanoSiO<sub>2</sub>. Addition of 0.5% NanoSiO<sub>2</sub> reduced the piezoresistive axial strain of smart cement by 16.5%. The compressive axial failure strain was 0.20%, so the piezoresistive axial strain has been increased by 1,670 times (167,000%) making the smart cement to be highly sensing. The model parameters  $q_2$  and  $p_2$  were 0.05 and 0.38 respectively. The coefficient of determination ( $R^2$ ) was 0.99 and the root-mean-square error (RMSE) was 0.021 MPa as summarized in Table 7.

**(c). Smart Cement with 1% NanoSiO<sub>2</sub>**

The piezoresistive axial strain of the smart cement with 1% NanoSiO<sub>2</sub> at failure  $\left(\frac{\Delta\rho}{\rho_o}\right)_f$  after 28 days of curing was 250%, as summarized in Table 7 and shown in Figure 9. Compressive piezoresistive axial strain at failure reduced by 41.6% after 28 days of curing and the percentage reduction was higher than the smart cement without NanoSiO<sub>2</sub>. Addition of 1% NanoSiO<sub>2</sub> reduced the piezoresistive axial strain of smart cement by 37.5%. The compressive axial failure strain was 0.19%, so the piezoresistive axial strain has been increased by 1,316 times (131,600%) making the smart cement to be highly sensing. The model parameters  $q_2$  and  $p_2$  were 0.35 and 0.14 respectively. The coefficient of determination ( $R^2$ ) was 0.99 and the root-mean-square error (RMSE) was 0.016 MPa as summarized in Table 7.

**Table 7. Piezoresistive axial strain at failure and Strength of the Smart Cement without and with NanoSiO<sub>2</sub> After 28 days of Curing**

Material	NanoSiO <sub>2</sub> (%)	Curing Time (day)	$\left(\frac{\Delta\rho}{\rho_o}\right)_f$ (%)	$\sigma_{cf}$ (MPa)	$p_2$	$q_2$	RMSE (MPa)	$R^2$
Smart Cement	0%	28	400 ± 10	19.3 ± 2	0.03 ± 0.02	0.05±0.03	0.022	0.99
	0.5%	28	334 ± 13	22.3 ± 3	0.38 ± 0.05	0.05±0.02	0.021	0.99
	1.0%	28	250 ± 8	27.5 ± 3	0.14 ± 0.02	0.35±0.03	0.016	0.99

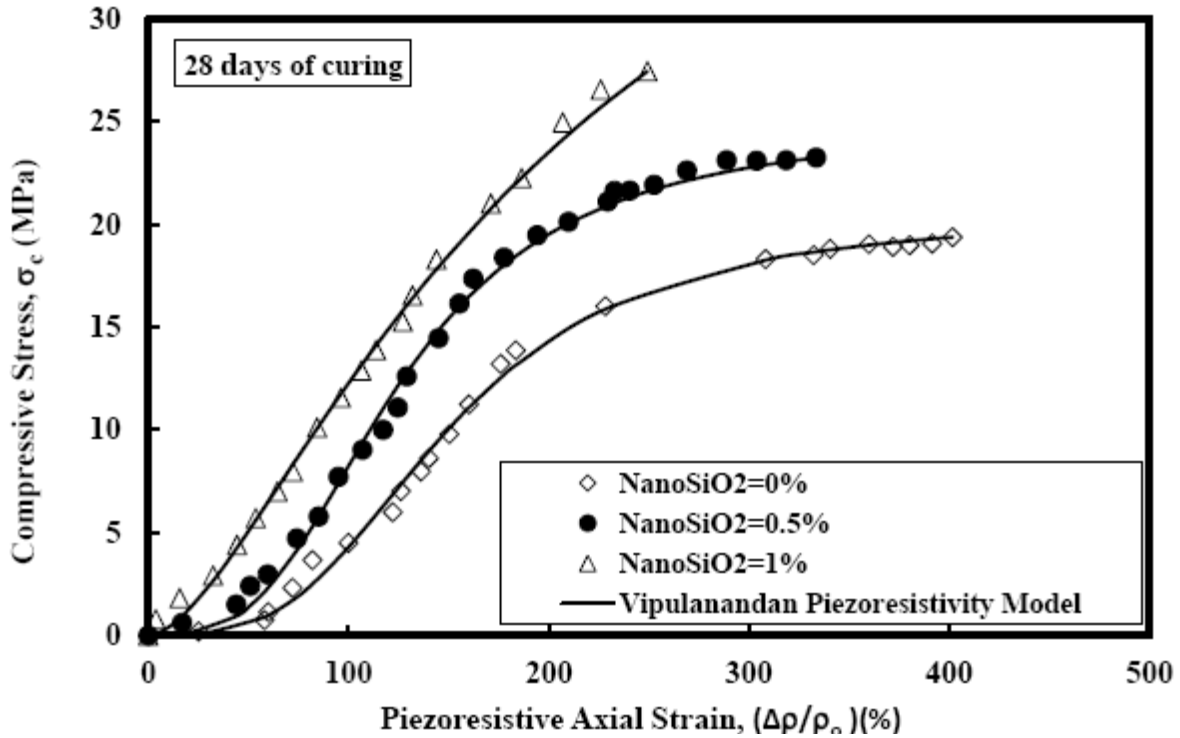


**Figure 9. Compressive Piezoresistive behavior of smart cement with various amount of NanoSiO<sub>2</sub> after 28 days of curing**

**Nonlinear model (NLM)**

The electrical resistivity ( $\rho$ ) of the smart cement slurry modified with silica nanoparticle (NanoSiO<sub>2</sub>) was influenced by the composition of the cement and curing time ( $t$  (day)). It is being proposed to relate the model parameters to the independent variables (curing time and NanoSiO<sub>2</sub> content) using a nonlinear power relationship (Vipulanandan et al. 2015 a). Hence the effects of curing time ( $t$ ) and NanoSiO<sub>2</sub> content on the model parameters were determined using the nonlinear model (NLM) (Vipulanandan et al. 2015a) as follows:

$$\text{Model parameters} = a*(t)^b + c*(t)^d *(NanoSiO_2(\%))^e \tag{9}$$

The NLM parameters (a, b, c, d, e) were obtained from multiple regression analyses using the least square method.

**(a). Piezoresistive Axial Strain at Failure  $\left(\frac{\Delta\rho}{\rho_0}\right)_f$**

Based on the nonlinear model parameter a (Eqn. (9)), curing time had the second highest effect on the parameter  $\left(\frac{\Delta\rho}{\rho_0}\right)_f$  compared to  $\sigma_f$ ,  $q_2$  and  $p_2$ . Based on the NLM parameter c, addition of NanoSiO<sub>2</sub> had the highest effect on the parameter  $\left(\frac{\Delta\rho}{\rho_0}\right)_f$  compared to  $\sigma_f$ ,  $q_2$  and  $p_2$  as summarized in Table 8.

**(b). Compressive Strength ( $\sigma_{cf}$ )**

Based on the nonlinear model parameter a (Eqn. (9)), curing time had the highest effect on increasing the parameter  $\sigma_{cf}$  compared to  $\left(\frac{\Delta\rho}{\rho_o}\right)_f$ ,  $q_2$  and  $p_2$ . Based on the NLM parameter c, addition of NanoSiO<sub>2</sub> had the highest effect on increasing the parameter  $\sigma_f$  compared to  $\left(\frac{\Delta\rho}{\rho_o}\right)_f$ ,  $q_2$  and  $p_2$  as summarized in Table 8.

**(c). Parameter  $p_2$**

Based on the nonlinear model parameter a (Eqn. (9)), curing time had the lowest effect on increasing the parameter  $p_2$  compared to  $\left(\frac{\Delta\rho}{\rho_o}\right)_f$ ,  $\sigma_f$  and  $q_2$ . Based on the NLM parameter c, addition of NanoSiO<sub>2</sub> had the lowest effect on decreasing the parameter  $q_2$  compared to  $\left(\frac{\Delta\rho}{\rho_o}\right)_f$ ,  $\sigma_f$  and  $q_2$  as summarized in Table 8.

**(d). Parameter  $q_2$**

Based on the nonlinear model parameter a (Eqn. (9)), curing time had the second lowest effect on increasing the parameter  $q_2$  compared to  $\left(\frac{\Delta\rho}{\rho_o}\right)_f$ ,  $\sigma_f$  and  $p_2$ . Based on the NLM parameter c, addition of NanoSiO<sub>2</sub> had the second lowest effect on increasing the parameter  $q_2$  compared to  $\left(\frac{\Delta\rho}{\rho_o}\right)_f$ ,  $\sigma_f$  and  $p_2$  as summarized in Table 8.

**Table 8 Nonlinear model parameters for the NanoSiO<sub>2</sub> modified smart cement**

Model Parameters	a	b	c	d	e	No. of Data	RMSE	R <sup>2</sup>
$(\Delta\rho/\rho_o)_f$ (%)	3.0	-0.45	447.8	-0.10	-0.02	8	33.75	0.83
$\sigma_f$ (MPa)	10.8	0.18	2.35	0.36	1.13	8	0.57	0.98
$p_2$	0.16	-0.32	0.04	0.4	2.52	8	0.01	0.86
$q_2$	0.23	-0.42	0.10	0.32	3.76	8	0.05	0.86

**Compressive Strength-Resistivity Index Relationship**

During the entire cement hydration process both the electrical resistivity and compressive strength of the cement increased gradually with the curing time. For cement pastes with various NanoSiO<sub>2</sub> content, the change in the resistivity was varied during the hardening. The cement paste without NanoSiO<sub>2</sub> had the highest electrical resistivity change ( $RI_{24hr}$ ), as summarized in Table 2. The linear relationships between ( $RI_{24hr}$ ) and the 1 day, 7 days and 28 days compressive strengths (MPa) as shown in Figure 10 are as follows:

$$\sigma_{1day} = -7 \times RI_{24hr} + 4066 \quad R^2=0.96 \quad (10)$$

$$\sigma_{7days} = -0.16 \times RI_{24hr} + 73 \quad R^2=0.90 \quad (11)$$

$$\sigma_{28days} = -0.05 \times RI_{24hr} + 28 \quad R^2=0.93 \quad (12)$$

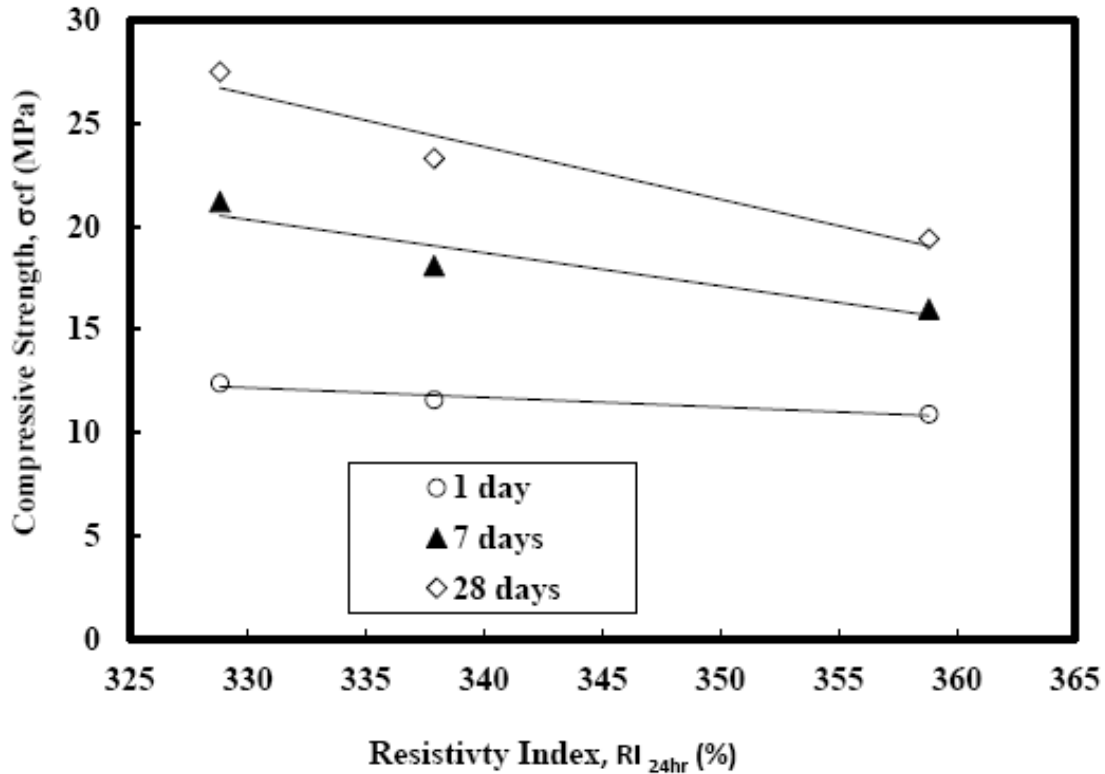


**Figure 10. Relationship between resistivity index ( $RI_{24hr}$ ) and compressive strength of smart cement modified with NanoSiO<sub>2</sub>**

## Conclusions

Based on the experimental and analytical study on the smart cement modified with silica nanoparticles (NanoSiO<sub>2</sub>) up to 1%, the following conclusions are advanced:

1. Based on the XRD analyses, with the addition of 1% NanoSiO<sub>2</sub>, changes in cement mineralogy was observed and the new constituents were magnesium silicate sulfate (Mg<sub>5</sub>(SiO<sub>4</sub>)<sub>2</sub>SO<sub>4</sub>) (2 $\theta$  peaks at 51.58° and 56.50°) and quartz (SiO<sub>2</sub>) (2 $\theta$  peaks at 23.55°, 36.90° and 62.50°). Hence some of the changes observed in the modified cement with NanoSiO<sub>2</sub> behavior could have been due to the changes in the cement mineralogy. TGA analyses also showed a great reduction in the total weight loss of the cement at 800°C when it's modified with 1% NanoSiO<sub>2</sub>.
2. Addition of 1% NanoSiO<sub>2</sub> increased the compressive strength of the smart cement by 14% and 42% after 1 day and 28 days of curing respectively. Also the modulus of elasticity of the smart cement increased with the additional of 1% NanoSiO<sub>2</sub>. Vipulanandan p-q stress-strain model predicted the behavior very well.
3. Resistivity was sensitive to the amount of NanoSiO<sub>2</sub> used to modify the smart cement. The amount of NanoSiO<sub>2</sub> can be detected based on the change in the initial resistivity. An addition of 1% NanoSiO<sub>2</sub> increased the initial electrical resistivity ( $\rho_0$ ) of smart cement by 35% and also increased the time to reach minimum resistivity by 31 minutes. Initial

electrical resistivity can be used as a good indicator for quality control. Vipulanandan p-q curing model predicted the behavior very well.

4. Addition of the NanoSiO<sub>2</sub> reduced the piezoresistivity (change the resistivity at peak stress) of the smart cement. Vipulanandan p-q piezoresistive model predicted the behavior very well.
5. Linear correlations were found between resistivity index (RI<sub>24</sub>) and compressive strength at different curing ages. Nonlinear model was used to correlate the model parameter to the curing time and NanoSiO<sub>2</sub> contents.

### Acknowledgements

This study was supported by the Center for Innovative Grouting Materials and Technology (CIGMAT) and Texas Hurricane Center for Innovative Technology (THC-IT) at the University of Houston, Houston, Texas with funding from various industries.

### References

1. Choolaei, M., Rashidi, A. M., Ardjmand, M., Yadegari, A. and Soltanian, H. (2012). The effect of nanosilica on the physical properties of oil well cement. *Materials Science and Engineering: A*, 538, 288-294.
2. Izon, D., Danenberger, E. P. and Mayes, M. (2007). Absence of fatalities in blowouts encouraging in MMS study of OCS incidents 1992-2006. *Drilling contractor*, 63(4), 84-89.
3. Labibzadeh, M., Zahabizadeh, B. and Khajehdezfuly, A. (2010). Early-age compressive strength assessment of oil well class G cement due to borehole pressure and temperature changes. *Journal of American Science*, 6(7), 1-7.
4. McCarter, W. J., Starrs, G. and Chrisp, T. M. (2000). Electrical conductivity, diffusion, and permeability of Portland cement-based mortars. *Cement and Concrete Research*, 30(9), 1395-1400.
5. McCarter, W. J., Chrisp, T. M., Starrs, G. and Blewett, J. (2003). Characterization and monitoring of cement-based systems using intrinsic electrical property measurements. *Cement and Concrete Research*, 33(2), 197-206.
6. Mohammed, S. (2016). Effect of temperature on the rheological properties with shear stress limit of iron oxide nanoparticle modified bentonite drilling muds. *Egyptian Journal of Petroleum*, 10.1016/j.ejpe.2016.10.018.
7. Han, B. and Ou, J. (2007). Embedded piezoresistive cement-based stress/strain sensor. *Sensors and Actuators A: Physical*, 138(2), 294-298.
8. Han, B., Zhang, L. Zhang, C., Wang, Y., Yu, X. and Ou, J. (2016). Reinforcement Effect and mechanism of Carbon Fibers to Mechanical and Electrically Conductive Properties of Cement-Based Materials, *Construction and Building materials*, Vol. 125, pp. 479-489.
9. Hou, P., Qian, J., Cheng, X. and Shah, S. P. (2015). Effects of the pozzolanic reactivity of nanoSiO<sub>2</sub> on cement-based materials. *Cement and Concrete Composites*, 55, 250-258.
10. Mangadlao, J. D., Cao, P. and Advincula, R. C. (2015). Smart cements and cement additives for oil and gas operations. *Journal of Petroleum Science and Engineering*, Vol. 129, 63-76.

11. Quercia, G., Brouwers, H. J. H., Garnier, A. and Luke, K. (2016). Influence of olivine nano-silica on hydration and performance of oil-well cement slurries. *Materials & Design*, 96, 162-170.
12. Singh, L. P., Karade, S. R., Bhattacharyya, S. K., Yousuf, M. M. and Ahalawat, S. (2013). Beneficial role of nanosilica in cement based materials–A review. *Construction and Building Materials*, 47, 1069-1077.
13. Vipulanandan, C. and Mohammed, A. (2015 a). Smart cement modified with iron oxide nanoparticles to enhance the piezoresistive behavior and compressive strength for oil well applications. *Smart Materials and Structures*, 24(12), 125020.
14. Vipulanandan, C, Mohammed, A., Boncan, V., Narvaez, G., Head, B. and Pappas, J. M. (2015b). Iron Nanoparticle Modified Smart Cement for Real Time Monitoring of Ultra Deepwater Oil Well Cementing Applications, OTC-25842-MS.
15. Vipulanandan, C. and Mohammed, A. (2017). Rheological Properties of Piezoresistive Smart Cement Slurry Modified With Iron-Oxide Nanoparticles for Oil-Well Applications. *Journal of Testing and Evaluation*, 45(6).
16. Vipulanandan, C., and Ali, K., (2018a) Smart Cement Grouts for Repairing Damaged Piezoresistive Cement and the Performances Predicted Using Vipulanandan Models, *Journal of Civil Engineering Materials*, American Society of Civil Engineers (ASCE), Vol. 30, No. 10, Article number 04018253.
17. Vipulanandan, C., and Amani, N., (2018b) Characterizing the Pulse Velocity and Electrical resistivity Changes In Concrete with Piezoresistive Smart Cement Binder Using Vipulanandan Models, *Construction and Building Materials*, Vol. 175, pp. 519-530.
18. Vipulanandan, C. (2021). *Smart Cement: Development, Testing, Modeling and Real-Time Monitoring*, CRC Press, Taylor and Francis, 440 pp.
19. Wei, X., Xiao, L. and Li, Z. (2012). Prediction of standard compressive strength of cement by the electrical resistivity measurement. *Construction and Building Materials*, 31, 341-346.